Available online at www.ijournalse.org

Emerging Science Journal

(ISSN: 2610-9182)

Vol. 6, No. 3, June, 2022

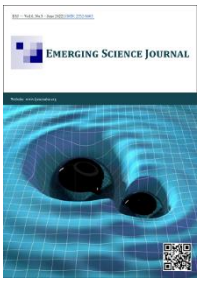

Hybrid Controller based on Null Space and Consensus Algorithms for Mobile Robot Formation

Gabriela M. Andaluz [1, 2], Paulo Leica [3], Marco Herrera [3], Luis Morales [3], Oscar Camacho [4*]

[1] *Universidad Internacional del Ecuador, Quito 170102,Ecuador.*

[2] *Department of Electronic Engineering and Communications, University of Zaragoza, 44003 Teruel, Spain.*

[3] *Departamento de Automatización y Control Industrial, Escuela Politénica Nacional, Quito 170517, Ecuador.*

[4] *Colegio de Ciencias e Ingenierías ¨El Politécnico", Universidad San Francisco de Quito USFQ, Quito 170157, Ecuador.*

Abstract

This work presents a novel hybrid control approach based on null space and consensus algorithms to solve the scalability problems of mobile robot formation and improve leader control through multiple control objectives. In previous works, the training of robots based on the null space requires a rigid training structure based on a geometric shape, which increases the number of agents in the formation. The scheme of the control algorithm, which does not make formation scalability possible, must be changed; therefore, seeking the scalability of training based on null space is a challenge that could be solved with the inclusion of consensus algorithms, which allow the control structure to be maintained despite increasing or decreasing the number of robot followers. Another advantage of this proposal is that the formation of the followers does not depend on any geometric figure compared to previous works based on the null space; this new proposal does not present singularities as if the structure is based on geometric shape, the latter one is crucial since the formation of agents can take forms that cannot be achieved with a geometric structure, such as collinear locations, that can occur in many environments. The proposed hybrid control approach presents three tasks: i) leader position task, ii) leader shape task, and iii) follower formation task. The proposed algorithm is validated through simulations, performing tests that use the kinematic model of non-holonomic mobile robots. In addition, linear algebra and Lyapunov theory are used to analyze the stability of the method.

Keywords:

Consensus Algorithms;
Distributed Control Algorithms;
Null-Space;
Mobile Robots;
Formation Scalability.

Article History:

Received:	02	October	2021
Revised:	26	February	2022
Accepted:	11	March	2022
Available online:	19	April	2022

1- Introduction

Mobile robotics is widely studied and is of interest to many researchers due to its wide field of application. The multi-robot mobile system allows the abilities of each mobile robot to be transferred as a contribution to the functionalities of a group of robots that interact with each other and makes it possible to work in teams to perform a common task. Some advantages of this structure are improvements in terms of performance, speed, efficiency, coordination, and execution of more complex tasks that a single robot could not perform [1, 2].

New approaches to address the autonomy of a robotic system through robot redundancy, that is, the extra degrees of freedom available to solve the main task, these approaches allow to cope with the increasing complexity of the robotic

* **CONTACT**: ocamacho@usfq.edu.ec

DOI: http://dx.doi.org/10.28991/ESJ-2022-06-03-01

© 2022 by the authors. Licensee ESJ, Italy. This is an open access article under the terms and conditions of the Creative Commons Attribution (CC-BY) license (https://creativecommons.org/licenses/by/4.0/).

systems and to exploit them to simultaneously solve a hierarchy of multiple tasks with different levels of priority [3]. In particular, the redundancy is addressed using the robot null-space for two different robotic systems and goals. The problem of controlling the position of a group of unicycle-type robots to follow in formation a time-varying reference, avoiding obstacles when needed, is presented by Martinez et al. (2021) [4]. It is proposed a kinematic control scheme that, unlike existing methods, can simultaneously solve both tasks involved in the problem, effectively combining control laws devoted to achieving formation tracking and obstacle avoidance. The main contributions of the paper are twofold: first, the advantages of the proposed approach are not all integrated into existing schemes, ours is fully distributed since the formulation is based on consensus, including the leader as part of the formation, scalable for many robots, generic to define the desired formation, and it does not require a global coordinate system or a map of the environment. Second, to the authors' knowledge, it is the first time that a distributed formation tracking control is combined with obstacle avoidance to solve both tasks simultaneously using a hierarchical scheme, thus guaranteeing continuous robot velocities despite activation/deactivation of the obstacle avoidance task, and stability is proven even in the transition of tasks. The effectiveness of the approach is shown through simulations and experiments with real robots. A comprehensive review of the leader-follower robotics system is presented by Rashid et al. (2019) [5]. The paper aims to find and elaborate on the current trends in the swarm robotic system, leader-follower, and multi-agent systems. Another part of this review focused on finding the trend of controllers utilized by previous researchers in the leader-follower system. The controllers that the researchers commonly apply are mostly adaptive and nonlinear controllers. The paper also explores the subject of study or system used during the research, which usually employs multi-robot, multi-agent, space-flying, reconfigurable, multi-legs, or unmanned systems. Another aspect of this paper concentrates on the topology employed by the researchers when they conduct simulation or experimental studies. A Lyapunov-based control law to achieve two multi-objective tasks for a network of open-loop unstable, non-holonomic mobile inverted pendulum (MIP) robots, using a connected undirected graph for inter-agent communication, using the first protocol, translationally invariant formations are achieved along with the synchronization of attitudes and heading velocities to desired values [6]. The control laws are based on the kinematic model of the mobile robot, and control torques for the MIPs are extracted using a two-loop control architecture. Both protocols guarantee the boundedness of the linear heading velocity, which is necessary for the stability of the two-loop control architecture. The proposed control laws are experimentally validated on indigenously built MIP robots.

Implementing several tasks in a single control algorithm is an advantage from the control point of view, which is why the implementation of algorithms based on null space has taken on great relevance. An algorithm of behaviors is used to execute tasks and sub-tasks of an autonomous robot system. These tasks are achieved simultaneously without generating conflict between them using the null space approach to execute lower hierarchy tasks [7]. The experimental results of the formation of multi-robot systems based on null spaces are shown in Antonelli et al. (2009) [8]. However, it does not consider the scalability of the formation. The null-space-based controller implementation is introduced to achieve multiple tasks within the heterogeneous formation of aerial and terrestrial robots [9]. However, in this proposal, the robot formation depends on a geometric shape. The formation of N-holonomic agents is solved using the hierarchical task-based scheme [10]; although, in that work, obstacle avoiding and agent formation are considered. Besides, a control algorithm with rigid and flexible formations to avoid static and dynamic obstacles is implemented in Leica et al. (2018) [11]. As proposed in Arevalo et al. (2018) [12], these do not consider human-robot interaction can control the formation. Previous works are applications with distributed control, where the control strategy must contemplate that the follower robots can move in a geometric space formed by other robots known as leaders. An adaptive null-space-based behavioral (NSB) method to deal with the problems of saturation planning and lack of adaptability when the traditional NSB method is applied to the formation control of multiple unmanned surface vehicles [13], a control strategy based on null-space for monitoring the trajectory of training of aerial manipulators in congested environments is shown in Camacho et al. (2019) [14]. By means of the null-space control, several control objectives can be achieved, assigning a priority to each of the objectives.

The strategy proposes controlling a homogeneous formation of three aerial manipulators for trajectory tracking and the evasion of obstacles. A null-space technique is used to guide the formation of two mobile robots autonomously; a differential drive wheeled ground vehicle and an unmanned aerial vehicle [15]. A controller based on Null-Space is used for the trajectory tracking of a formation of three quadcopters to evade grounded and aerial mobile obstacles [16]. A formation of robots based on null space, where the robot formation depends on a geometric figure, hinders the scalability of the robot formation [17]. An unmanned ground vehicle (UGV) and an unmanned aerial vehicle (UAV) use the concepts of null space control by robot formation [18]. A controller to autonomously guide a rigid formation of two mobile robots, a wheeled land vehicle with a differential drive, and an unmanned aerial vehicle, based on null space, is presented in [15, 19]. The problem of multi-agent formation with trajectory tracking and obstacle avoidance, the formation control based on null-space, is considered in [20, 21]. In the previous works based on Null-Space, the robot formation depends on a geometric figure, which hinders the scalability of the robot formation.

Null-space algorithms solve the inconvenience of multiple tasks, however with this control strategy, performing the training of several robots implies several disadvantages: i) it is necessary to change the shape and posture matrices, as

well as their Jacobians, ii) there are configurations in the formation that present singularities, for example, the robots cannot be located collinearly with each other, iii) the calculation of the centroid of the formation becomes more complex, and in the cases of collinear robots, it cannot be calculated. For all the above, it is necessary to look for an alternative that improves the characteristics of the robot formation. The consensus algorithms allow avoiding singularities in the formation. Using leading virtual robots allows calculating the centroid of the formation simply and does not require the change of the posture and form matrices as it happens in the null space algorithm.

Consensus algorithms have been implemented in multi-vehicle cooperative control as presented in [22–24]. A robot could be represented by a double integrator dynamic model [25]. A distributed control algorithm is developed to drive the multi-robot system to follow a group of dynamic leaders with containment and group dispersion behaviors. A distributed containment control for double-integrator dynamics in the presence of both stationary and dynamic leaders, where the control of leaders becomes complex and does not allow to control the orientation or form of the formation [26, 27]. Consensus algorithms are implemented to track the trajectory of a group of robots; however, neither the shape nor the position of the formation can be controlled [28]. A decentralized adaptive controller to cooperatively manipulate a payload of unknown mass employing multiple aerial robots is presented by Moreira et al. (2019) [15], where consensus algorithms are used to ensure that the manipulated load can be evenly distributed in each agent; its speed is constant converges to the given reference. The multi-agent system formation scaling control problem is studied in [13], where only one agent knows the desired formation size. In that work, the authors design a formation scaling control for universally rigid frameworks using the stress matrix; however, this work does not consider that robot formation can perform multiple subtasks.

The consensus algorithm is used for the coordinated motion control of a wheel-leg robot [29]. A formation control strategy merges the formation control algorithm, consensus control algorithm, and artificial potential field algorithm [30]. The formation control algorithm controls the formation of multiple robot formations. A consensus algorithm for distributed cooperative formation trajectory planning is proposed by combining improved artificial potential field and consensus theory [31]. A quadrotor variable formation control method based on a consensus control algorithm is proposed by Xu et al. (2020) [32]. A comparison between sliding mode and consensus approaches for quadrotor leader-follower formation flight [33]. Finally, a distributed consensus algorithm for second-order nonlinear multi-agent systems is formulated under the leader-following approach [34]. The consensus algorithms allow formations without singularities; another advantage is that they do not require a geometric shape to perform the formation of the followers; however, they require algorithms for the formation of the leading robots, and it is complex to perform a posture and shape control to the leaders. Therefore, it is necessary to have several control objectives. That is why a novel hybrid combination of consensus and null space algorithms is carried out to take advantage of both control strategies.

On the one hand, the consensus algorithms allow eliminating the dependence on geometric shapes to form followers and avoid singularities that occur in geometric shapes. In contrast, the null space allows several control objectives to be carried out in a single control strategy, such as controlling the leader form and posture and controlling the formation of the follower robots. Another advantage of this hybrid algorithm is the scalability given to the null space.

The main contributions of this manuscript can be enumerated as follows:

- A hybrid control topology combining the null space approach and consensus algorithms is presented.
- The hybrid control topology enhances multitasking in the formation of mobile robots regardless of the number of robots.
- The formation of the follower robots as a task within the null space does not depend on a geometric figure, so it is not necessary to redesign the controller, introducing scalability to the null space, adding advantages to the hybrid proposal.
- With this proposal, the singularities generated in certain configurations of the formation of the robot followers are avoided.

This paper is organized as follows: In section 2, the modeling of mobile robot formation is presented. Then, the control design based on the consensus algorithm and null-space approach for robot mobile formation is developed in section 3. Then, in section 4, the simulation results are shown. Finally, the conclusions are given in section 5.

2- Research Methodology

This paper presents a hybrid control strategy based on consensus and null space algorithms. Figure 1 shows the outline of the research methodology. The system initializes when the shape and posture parameters of the leader robots are defined. These parameters are used in the null space algorithm. This algorithm performs three tasks: i) Task 1: performs a posture control of the leader robots. They form a square geometric figure; the centroid of this geometric figure is identified, and the Jacobian of posture is determined. After this, the control actions are generated so that the centroid of the formation of the leader robots follows the desired trajectory. ii) Task 2: a shape control is applied to the

leader robots; the geometric shape of these robots is described; in this case, the shape is a square. Then the Jacobian of shape is defined, and the control actions are generated so that the leader robots form the desired geometric figure. iii) Task 3: A consensus algorithm is implemented for the formation of the robot followers. The Laplacian formation matrix is defined according to the number of existing robot followers. Finally, control actions are produced for the follower robots to take the desired positions in the robot formation. Consider that the control algorithms constantly require information about the positions of the leader and follower robots.

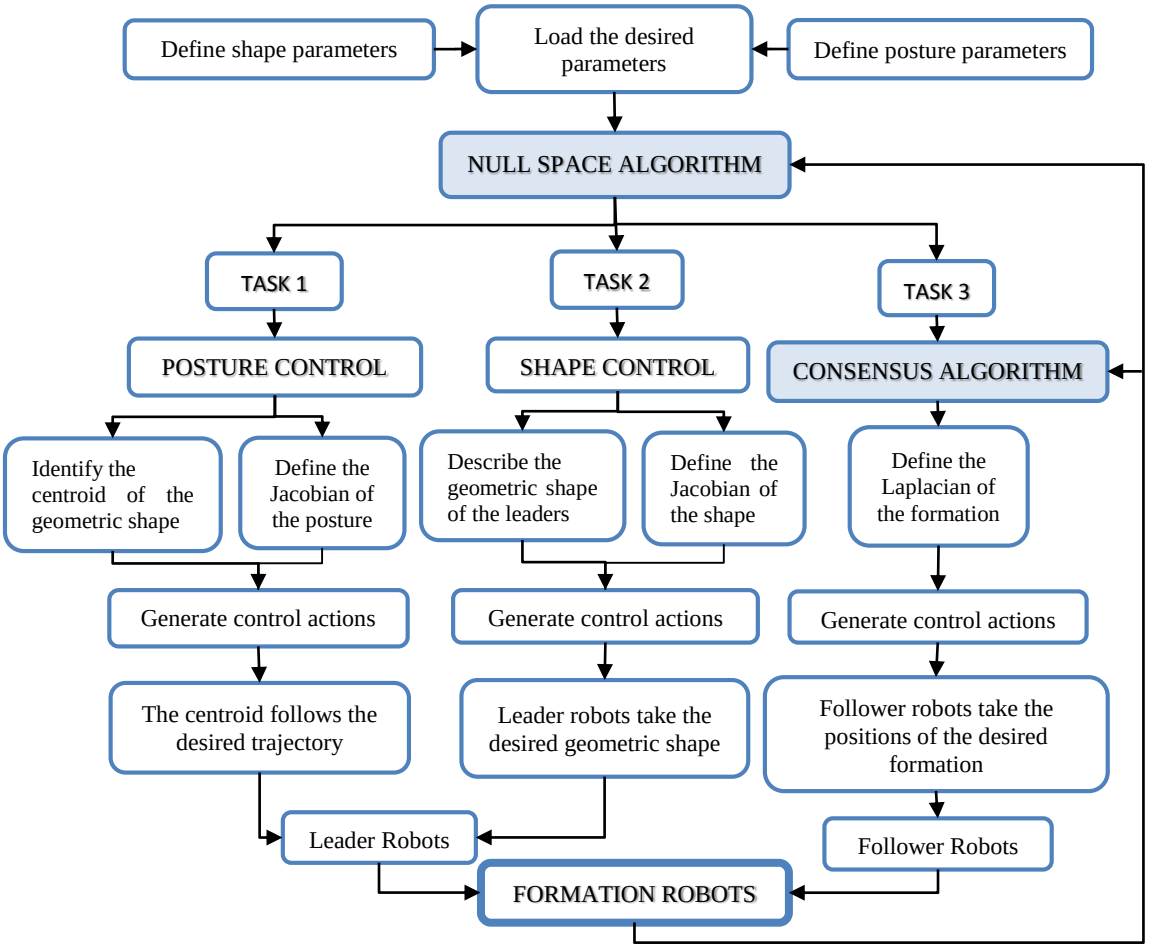

Figure 1. Flowchart of hybrid control

3- Model Robot

In Figure 2, a mobile differential traction robot is shown.

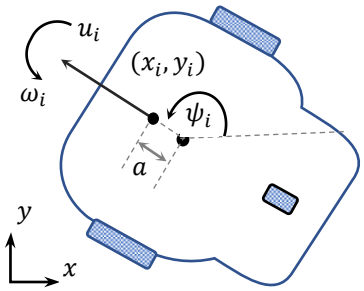

Figure 2. Differential traction mobile robot

In the present work differential drives, mobile robots with non-holonomic restriction are used; the kinematic model is given by [6]:

$$\dot{X}_i = \begin{bmatrix} \cos(\psi_i) & -a\cos(\psi_i) \\ \sin(\psi_i) & a\cos(\psi_i) \\ 0 & 1 \end{bmatrix} \begin{bmatrix} u_i \\ \omega_i \end{bmatrix} = J_{ri} U_i \quad (1)$$

where $\dot{X}_i = [\dot{x}_i \;\; \dot{x}_j]$ are the temporal variations of the position X and Y of the *i-th* robot, Ψ_i is its orientation u_i, and ω_i are its linear and angular velocities respectively, and J_{Ri} is its Jacobian. Thus, for n robots, the kinematics model is defined by:

$$\dot{h} = J_R U \tag{2}$$

where $\dot{h} = [\dot{x}_{R1} \;\; \dot{y}_{R1} \;\; \dot{x}_{R2} \;\; \dot{y}_{R2} \ldots \dot{x}_{Ri} \;\; \dot{y}_{Ri}]$; $U = [u_1 \;\; \omega_1 \;\; u_2 \;\; \omega_2 \cdots u_i \;\; \omega_i]$ with;

$$J_R = \begin{bmatrix} J_{R1} & 0 & 0 & 0 \\ 0 & J_{R2} & 0 & 0 \\ 0 & 0 & \ddots & 0 \\ 0 & 0 & 0 & J_{Rn} \end{bmatrix}$$

3-1- Null-Space Algorithms

Figure 3 presents the scheme of the formation control based on null space, where the system must carry out three tasks: ***Task 1:*** To maintain the position of leader robots; ***Task 2:*** To maintain the shape of leader robots.

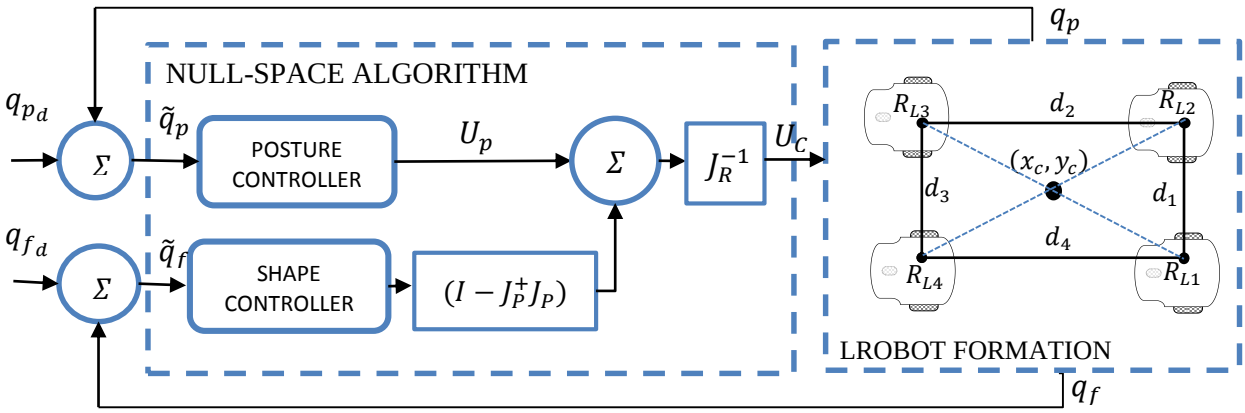

Figure 3. Null-space control structure

Figure 4 shows the formation of leader robots; where $R_{L1} = [x_{L1} \;\; y_{L1}]$, $R_{L2} = [x_{L2} \;\; y_{L2}]$, $R_{L3} = [x_{L3} \;\; y_{L3}]$, and $R_{L4} = [x_{L4} \;\; y_{L4}]$ are the positions of the leader robots; $[x_c \;\; y_c]$ is the position of the centroid of the formation; d_1, d_2, d_3, and d_4 are the distances between robots. The shape variable q_f is represented by:

$$q_f = \begin{bmatrix} d_1 \\ d_2 \\ d_3 \\ d_4 \end{bmatrix} = \begin{bmatrix} \sqrt{(x_{L1} - x_{L2})^2 + (y_{L1} - y_{L2})^2} \\ \sqrt{(x_{L2} - x_{L3})^2 + (y_{L2} - y_{L3})^2} \\ \sqrt{(x_{L3} - x_{L4})^2 + (y_{L3} - y_{L4})^2} \\ \sqrt{(x_{L4} - x_{L1})^2 + (y_{L4} - y_{L1})^2} \end{bmatrix} \tag{3}$$

The posture variable q_p is defined by:

$$q_p = \begin{bmatrix} x_c \\ y_c \end{bmatrix} = \begin{bmatrix} \dfrac{x_{L1} + x_{L2} + x_{L3} + x_{L4}}{4} \\ \dfrac{y_{L1} + y_{L2} + y_{L3} + y_{L4}}{4} \end{bmatrix} \tag{4}$$

The control law is defined by:

$$U_c = J_R^{-1}\{U_p + J_2 U_f\} \tag{5}$$

where: $J_2 = (I - J_p^+ J_p)$

$$U_f = J_f^+ \left\{ \dot{q}_{fd} + K_f \tanh \frac{K_{f1} \tilde{q}_f}{K_f} \right\} \tag{6}$$

$$U_p = J_p^{+}\left\{\dot{q}_{pd} + K_p \tanh\frac{K_{p1}\tilde{q}_p}{K_p}\right\} \tag{7}$$

where, K_f, K_{f1}, $K_{p,}$ and K_{p1} are positive constants for the tuning of the controller. $\tilde{q}_f$ and $\tilde{q}_p$ are the form the shape errors, respectively. $\dot{q}_{fd}$ and $\dot{q}_{pd}$ are the time derivates of the desired variables of form and posture.

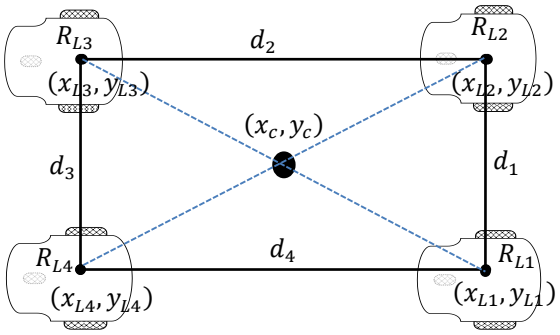

Figure 4. Leader robot formation

3-2- Consensus Algorithms

In Figure 5, a control algorithm structure is shown.

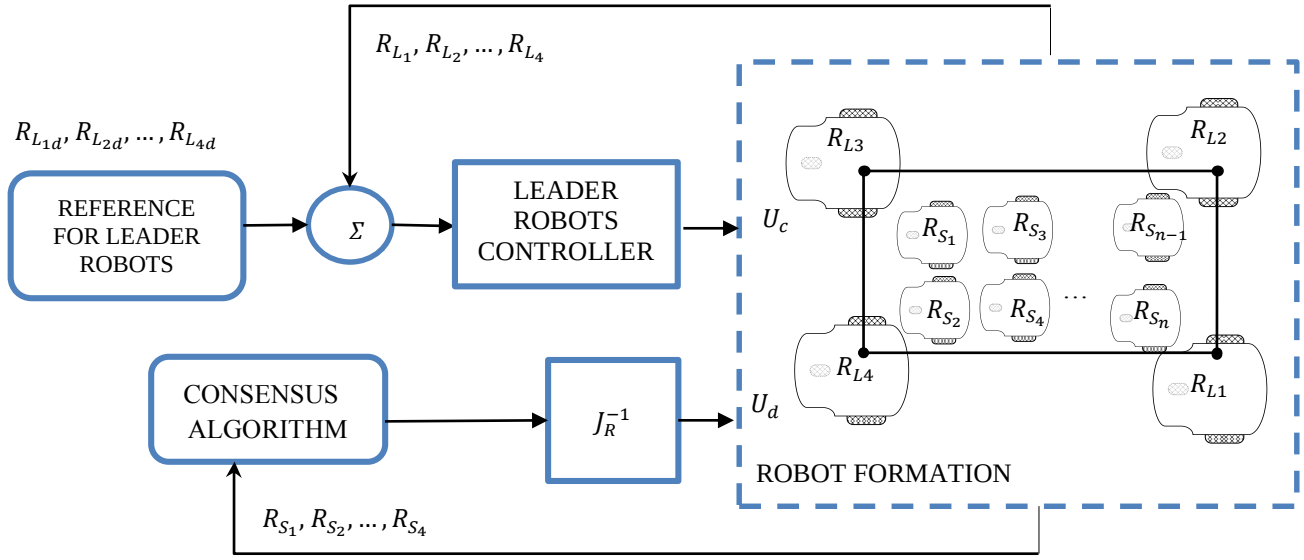

Figure 5. Control algorithm structure

The consensus algorithm control law according to [20] is expressed as:

$$\ddot{X} = -\Gamma X - \alpha\Gamma\dot{X} - \beta\,\mathrm{sgn}\left(\gamma\,\Gamma X + \Gamma\dot{X}\right) + \psi_x \tag{8}$$

$$\ddot{Y} = -\Gamma Y - \alpha\Gamma\dot{Y} - \beta\,\mathrm{sgn}\left(\gamma\,\Gamma Y + \Gamma\dot{Y}\right) + \psi_y \tag{9}$$

where Γ is the Laplacian matrix, X and Y are the robot positions $\dot{X} = [\dot{x}_{L1}\ \dot{x}_{L2} \ldots \dot{x}_{L4}\ \dot{x}_{s1}\ \dot{x}_{s2} \cdots \dot{x}_{sn}]^T$, $\dot{Y} = [\dot{y}_{L1}\ \dot{y}_{L2} \ldots \dot{y}_{L4}\ \dot{y}_{s1}\ \dot{y}_{s2} \cdots \dot{y}_{sn}]^T$ are the derivatives of the position of the robots, $\ddot{X}$ and $\ddot{Y}$ are the second derivatives in the x-y axis of the leader and followers robots. α, β and γ are controller scaling gains Ψ_x and Ψ_y accelerations in the leader robots x-y axis. Due to the robots input being input with only one derivative and the consensus control law having a double derivative, the control law is integrated through the Euler method.

$$\dot{X} = \ddot{X}\,t_s + \dot{X}_{k-1} \tag{10}$$

$$\dot{Y} = \ddot{Y}\,t_s + \dot{Y}_{k-1} \tag{11}$$

where $\dot{X}_{k-1}$ and $\dot{Y}_{k-1}$ re the previous state, t_s is the sampling time, the control action for each robot is given by the inverse kinematics expressed as:

$$U_D = J_R^{-1}\begin{bmatrix} \dot{X}\, t_s + \dot{X}_{k-1} \\ \dot{Y}\, t_s + \dot{Y}_{k-1} \end{bmatrix} \tag{12}$$

Replacing Equations 8 and 9 in Equation 12, the control law is defined by:

$$U_D = J_R^{-1}\begin{bmatrix} \left\{-\Gamma X - \alpha\Gamma\dot{X} - \beta\,\mathrm{sgn}\left(\gamma\,\Gamma X + \Gamma\dot{X}\right) + \Psi_x\right\} t_s + \dot{X}_{k-1} \\ \left\{-\Gamma Y - \alpha\Gamma\dot{Y} - \beta\,\mathrm{sgn}\left(\gamma\,\Gamma Y + \Gamma\dot{Y}\right) + \Psi_y\right\} t_s + \dot{Y}_{k-1} \end{bmatrix} \tag{13}$$

3-3- Hybrid Algorithm (Consensus and Null-Space)

Figure 6 presents the scheme hybrid algorithm, where the system must carry out three tasks:

- Task 1: To maintain the position of leader robots.
- Task 2: To maintain the shape of leader robots.
- Task 3: To maintain the formation of follower robots.

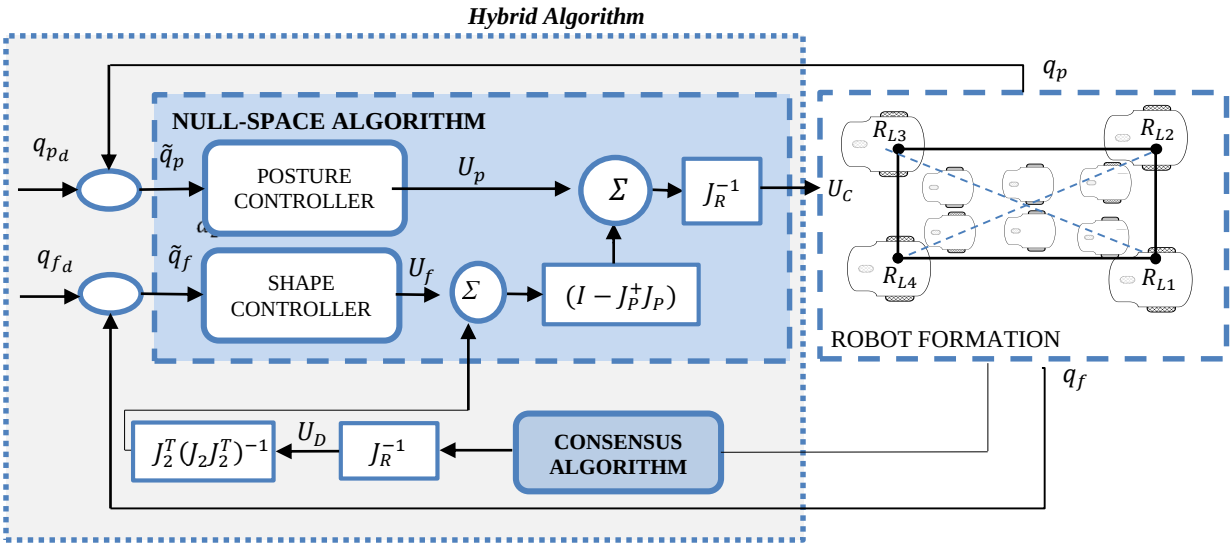

Figure 6. Hybrid algorithm (consensus and null-space)

Figure 7 shows the position of leaders and follower robots.

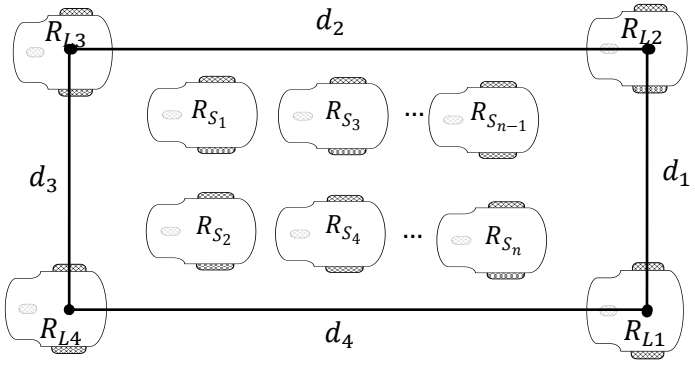

Figure 7. Position of the leaders and follower robots

R_{L1}, R_{L2}, R_{L3}, and R_{L4} are the leader position vectors; R_{S1}, R_{S2}, R_{S3} … $R_{Sn\text{-}1}$, and R_{Sn} are the position vectors of the followers. The kinematic posture model considering leaders and followers is given by:

$$\dot{q}_p = J_p \dot{h} \tag{14}$$

where $\dot{h} = [\dot{x}_{L1}\ \dot{y}_{L1} \ldots \dot{x}_{L4}\ \dot{y}_{L4}\ \dot{x}_{s1}\ \dot{y}_{s1}\ \dot{x}_{s2}\dot{y}_{s2}\ \cdots \dot{x}_{sn}\ \dot{y}_{sn}]^T$; $\dot{q}_p = [\dot{x}_c\ \dot{y}_c]^T$ moreover, the posture Jacobian is given by:

$$J_p = \begin{bmatrix} \frac{\partial x_c}{\partial x_{L1}} & \frac{\partial x_c}{\partial y_{L1}} & \frac{\partial x_c}{\partial x_{L2}} & \cdots & \frac{\partial x_c}{\partial x_{S1}} & \frac{\partial x_c}{\partial y_{S1}} & \cdots & \frac{\partial x_c}{\partial x_{Sn}} & \frac{\partial x_c}{\partial y_{Sn}} \\ \frac{\partial y_c}{\partial x_{L1}} & \frac{\partial y_c}{\partial y_{L1}} & \frac{\partial y_c}{\partial y_{L2}} & \cdots & \frac{\partial y_c}{\partial x_{S1}} & \frac{\partial y_c}{\partial y_{S1}} & \cdots & \frac{\partial y_c}{\partial x_{Sn}} & \frac{\partial y_c}{\partial y_{Sn}} \end{bmatrix} \quad (15)$$

The kinematic shape model is given by:

$$\dot{q}_f = J_f \dot{h} \quad (16)$$

where $\dot{q}_f = [\dot{d}_1 \ \dot{d}_2 \ \dot{d}_3 \ \dot{d}_4]$;

$$J_f = \begin{bmatrix} \frac{\partial d_1}{\partial x_{L1}} & \frac{\partial d_1}{\partial y_{L1}} & \frac{\partial d_1}{\partial x_{L2}} & \cdots & \frac{\partial d_1}{\partial x_{S1}} & \frac{\partial d_1}{\partial y_{S1}} & \cdots & \frac{\partial d_1}{\partial x_{Sn}} & \frac{\partial d_1}{\partial y_{Sn}} \\ \frac{\partial d_2}{\partial x_{L1}} & \frac{\partial d_2}{\partial y_{L1}} & \frac{\partial d_2}{\partial x_{L2}} & \cdots & \frac{\partial d_2}{\partial x_{S1}} & \frac{\partial d_2}{\partial y_{S1}} & \cdots & \frac{\partial d_2}{\partial_{Sn}} & \frac{\partial d_2}{\partial y_{Sn}} \\ \frac{\partial d_3}{\partial x_{L1}} & \frac{\partial d_3}{\partial y_{L1}} & \frac{\partial d_3}{\partial x_{L2}} & \cdots & \frac{\partial d_3}{\partial x_{S1}} & \frac{\partial d_3}{\partial y_{S1}} & \cdots & \frac{\partial d_3}{\partial_{Sn}} & \frac{\partial d_3}{\partial y_{Sn}} \\ \frac{\partial d_4}{\partial x_{L1}} & \frac{\partial d_4}{\partial y_{L1}} & \frac{\partial d_4}{\partial x_{L2}} & \cdots & \frac{\partial d_4}{\partial x_{S1}} & \frac{\partial d_4}{\partial y_{S1}} & \cdots & \frac{\partial d_4}{\partial_{Sn}} & \frac{\partial d_4}{\partial y_{Sn}} \end{bmatrix} \quad (17)$$

Taking into consideration the control objectives, the null space is defined by:

$$U_{cH} = J_R^{-1}\left\{U_p + J_2\left(U_f + J_2^{+}U_D\right)\right\} \quad (18)$$

where $J_2 = \left(I - J_p^{+}J_p\right)$; $J_2^{+} = (J_2 J_2^{T})^{-1}$.

$$U_f = J_f^{+}\left\{\dot{q}_{fd} + K_f \tanh\frac{K_{f1}\tilde{q}_f}{K_f}\right\} \quad (19)$$

$$U_p = J_p^{+}\left\{\dot{q}_{pd} + K_p \tanh\frac{K_{p1}\tilde{q}_p}{K_p}\right\} \quad (20)$$

where, K_f, K_{f1}, K_p and K_{p1} are positive constants for the tuning of the controller. $\tilde{q}_f$ and $\tilde{q}_p$ are the form and the shape errors, respectively.

$$U_D = \begin{bmatrix} \left\{-\Gamma X - \alpha\,\Gamma\dot{X} - \beta\,\mathrm{sgn}\left(\gamma\,\Gamma X + \Gamma\dot{X}\right) + \Psi_x\right\}t_s + \dot{X}_{k-1} \\ \left\{-\Gamma Y - \alpha\,\Gamma\dot{Y} - \beta\,\mathrm{sgn}\left(\gamma\,\Gamma Y + \Gamma\dot{Y}\right) + \Psi_y\right\}t_s + \dot{Y}_{k-1} \end{bmatrix} \quad (21)$$

where $J_p^{+} = J_p^{T}\left(J_p J_p^{T}\right)^{-1}$ and $J_f^{+} = J_f^{T}\left(J_f J_f^{T}\right)^{-1} J_f^{T}$.

3-4- Stability Analysis

In this subsection, the stability of the first task (posture) is analyzed. The posture kinematics is given by: $\dot{q}_p = J_p\dot{h}$, where $\dot{h} = [\dot{x}_{L1} \ \dot{y}_{L1} \ldots \dot{x}_{L4} \ \dot{y}_{L4} \ \dot{x}_{s1} \dot{y}_{s1} \ \dot{x}_{s2}\dot{y}_{s2} \ \cdots \dot{x}_{s3}]^T$; and $\dot{q}_p = [\dot{x}_c \ \dot{y}_c]$. By replacing the robot model:

$$\dot{q}_p = J_p\dot{h} = J_p J_R U \quad (22)$$

Assuming perfect velocity tracking $U=U_c$; in closed loop:

$$\dot{q}_p = J_p\left\{U_p + J_2\left(U_f + J_2^{+}U_D\right)\right\} \quad (23)$$

Replacing $J_2 = \left(I - J_p^{+}J_p\right)$ and knowing that: $J_p^{+} = J_p^{T}\left(J_p J_p^{T}\right)^{-1}$; thus $J_p J_p^{+} = I$; and expanding:

$$\dot{q}_p = J_p U_p \quad (24)$$

Replacing U_p and expanding:

$$\dot{q}_p = J_p J_p^+ \left\{ \dot{q}_{pd} + K_p \tanh \frac{K_{p1} \tilde{q}_p}{K_p} \right\} \tag{25}$$

$$\dot{\tilde{q}} + K_p \tanh \frac{K_{p1} \tilde{q}_p}{K_p} = 0 \tag{26}$$

Thus, if *Kp* and *Kp1* are positive constants $\tilde{q}_p \to 0$ with $t \to \infty$.

The stability of the second task is analyzed, the shape kinematics (shape of the leaders) is given by $\dot{q}_f = J_f \dot{h}$. Replacing the robot model:

$$\dot{q}_f = J_f J_R U \tag{27}$$

Assuming perfect velocity tracking $U=U_c$; in closed loop:

$$\dot{q}_f = J_f U_p + J_f J_2 \left(U_f + J_2^+ U_D \right) \tag{28}$$

Multiplying both members of the equation by: $J_f^+ = \left(J_f J_f^T \right)^{-1} J_f^T$ and considering that $J_f^+ J_f = I$:

$$J_f^+ \dot{q}_f = U_p + J_2 \left(U_f + J_2^+ U_D \right) \tag{29}$$

Replacing U_p and $J_2 = \left(I - J_p^+ J_p \right)$.

$$J_f^+ \dot{q}_f = J_p^+ \left\{ \dot{q}_{pd} + K_p \tanh \frac{K_{p1} \tilde{q}_p}{K_p} \right\} + \left(U_f + J_2^+ U_D \right) - J_p^+ J_p \left(U_f + J_2^+ U_D \right) \tag{30}$$

Multiplying both members of the equation by J_2:

$$J_2 J_f^+ \dot{q}_f = J_p^+ \left\{ \dot{q}_{pd} + K_p \tanh \frac{K_{p1} \tilde{q}_P}{K_p} \right\} + J_2 \left(U_f + J_2^+ U_D \right) - J_2 J_2^+ J_p \left(U_f + J_2^+ U_D \right) \tag{31}$$

by orthogonality $J_2 J_p^+ = 0$;

$$J_f^+ \dot{q}_f = U_f + J_2^+ U_D \tag{32}$$

Multiplying both members of the equation by J_p and by orthogonality $J_p J_2^+ = 0$.

$$J_f^+ \dot{q}_f = U_f \tag{33}$$

Replacing U_f:

$$J_f^+ \dot{q}_p = J_f^+ \left\{ \dot{q}_{fd} + K_f \tanh \frac{K_{f1} \tilde{q}_p}{K_f} \right\} \tag{34}$$

$$\dot{\tilde{q}}_f + K_f \tanh \frac{K_{f1} \tilde{q}_f}{K_f} = 0 \tag{35}$$

If K_f and K_{f1} are positive constants, then $\tilde{q}_f \to 0$ with $t \to \infty$. The stability of the third task (formation of the follower robots) is analyzed, the formation kinematics of the followers and leaders is given by:

$$h = J_R U$$

where $\dot{h} = [\dot{x}_{L1} \ \dot{y}_{L1} \ldots \dot{x}_{L4} \ \dot{y}_{L4} \ \dot{x}_{s1} \dot{y}_{s1} \ \dot{x}_{s2} \dot{y}_{s2} \ \cdots \dot{x}_{s3}]^T$.

Assuming perfect velocity tracking $U=U_c$; in closed loop:

$$\dot{h} = U_p + J_2 \left(U_f + J_2^+ U_D \right) \tag{36}$$

where: $J_2 J_2^+ = I$;

$$\dot{h} = U_p + J_2 U_f + U_D \tag{37}$$

Multiplying both members of the equation by J_p

$$J_p\dot{h} = J_pU_p + J_pJ_2U_f + J_pU_D \tag{38}$$

by orthogonal $J_pJ_2 = 0$

$$\dot{h} = U_p + U_D \tag{39}$$

Replacing U_p from Equation 20 and expanding Equation 39, it is obtained:

$$\dot{h} = J_p^+\{\dot{q}_{pd} + K_p \tanh\tilde{q}_p\} + U_D \tag{40}$$

Multiplying both members of Equation 40 by J_2, and by orthogonality $J_2J_p^+ = 0$, then:

$$\dot{h} = U_D \tag{41}$$

The control law U_D is:

$$\dot{h} = \begin{bmatrix} \{-\Gamma X - \alpha\Gamma\dot{X} - \beta\,\mathrm{sgn}(\gamma\,\Gamma X + \Gamma\dot{X}) + \Psi_x\}t_s + \dot{X}_{k-1} \\ \{-\Gamma Y - \alpha\Gamma\dot{Y} - \beta\,\mathrm{sgn}(\gamma\,\Gamma Y + \Gamma\dot{Y}) + \Psi_y\}t_s + \dot{Y}_{k-1} \end{bmatrix} \tag{42}$$

where $\dot{h} = [\dot{X}\ \dot{Y}]$ replacing and expanding, thus $\dot{h}$ can be rewritten as:

$$\begin{bmatrix} \dot{X} \\ \dot{Y} \end{bmatrix} = \begin{bmatrix} \{-\Gamma X - \alpha\Gamma\dot{X} - \beta\,\mathrm{sgn}(\gamma\,\Gamma X + \Gamma\dot{X}) + \Psi_x\}t_s + \dot{X}_{k-1} \\ \{-\Gamma Y - \alpha\Gamma\dot{Y} - \beta\,\mathrm{sgn}(\gamma\,\Gamma Y + \Gamma\dot{Y}) + \Psi_y\}t_s + \dot{Y}_{k-1} \end{bmatrix} \tag{43}$$

Replacing Equations 10 and 11, and expanding Equation 42, thus can be rewritten as:

$$\ddot{X} = -\Gamma X - \alpha\Gamma\dot{X} - \beta\,\mathrm{sgn}(\gamma\,\Gamma X + \Gamma\dot{X}) + \psi_x \tag{44}$$

It is known that ΓX the position error can be defined as $\Gamma X = \tilde{X}$ where $\tilde{X}$ is the position error on the x-axis. Therefore, it can be rewritten as:

$$X = \Gamma^{-1}\tilde{X} \tag{45}$$

By replacing Equation 42 and its temporal derivatives in Equation 41:

$$\ddot{\tilde{X}} = -\Gamma\dot{\tilde{X}} - \alpha\,\Gamma\ddot{\tilde{X}} - \beta\,\Gamma\,\mathrm{sgn}(\gamma\,\dot{\tilde{X}} + \ddot{\tilde{X}}) + \psi_x \tag{46}$$

For the stability analysis, it can be considered that the first n-m inputs corresponding to the four leaders are equal to zero since the consensus algorithm will be used to carry out the formation of the followers. The formation of the leaders is carried out in the second task. Thus, it can be rewritten in a simplified form as:

$$\dddot{\tilde{X}}_F = -M\ddot{\tilde{X}}_F - \alpha M\dddot{\tilde{X}}_F - \beta M\,\mathrm{sgn}(\gamma\ddot{\tilde{X}}_F + \dddot{\tilde{X}}_F) + \psi_F \tag{47}$$

where $\Psi_F = \Gamma\Psi_x$ are position vector error in X, Y., velocity vectors error in x and y. , and leader acceleration vectors in x and y. To find a candidate function to test the stability criterion, the matrices P and Q are defined as:

$$P = \begin{bmatrix} I_m & \gamma M^{-1} \\ \gamma\,M^{-1} & M^{-1} \end{bmatrix} \tag{48}$$

$$Q = \begin{bmatrix} \gamma\,I_m & \dfrac{\alpha\gamma}{2}I_m \\ \dfrac{\alpha\gamma}{2}I_m & \alpha I_m - \gamma M^{-1} \end{bmatrix} \tag{49}$$

where I_m is an $m \times m$ identity matrix, $M = [m_{ij}] \in R^{m\times m}\ m_{ij} = l_{ij}$ defined as the Laplacian matrix. Since the mentioned matrices are symmetrical, to define them as positive, their eigenvalues must be positive. To achieve this, the following conditions must be met:

$$\gamma < \sqrt{\lambda_{\min}(M)} \text{ and } \gamma < \frac{4\alpha\lambda_{\min}(M)}{4+\alpha^2\lambda_{\min}(M)}$$

where $\lambda_{min}(M)$ is the smallest eigenvalue of M. According to which the Lyapunov candidate function is defined as follow:

$$V = \frac{1}{2}\tilde{X}_F^T\tilde{X}_F + \gamma\,\tilde{X}_F^T M^{-1}\tilde{X}_F + \frac{1}{2}\tilde{X}_F^T M^{-1}\tilde{X}_F \tag{50}$$

Deriving V, it is obtained:

$$\dot{V} = -\begin{bmatrix}\tilde{X}_F^T & \tilde{X}_F\end{bmatrix} Q \begin{bmatrix}\tilde{X}_F^T \\ \tilde{X}_F\end{bmatrix} - \beta\left(\gamma\,\tilde{X}_F + \tilde{X}_F\right)^T \operatorname{sgn}\left(\gamma\,\tilde{X}_F + \tilde{X}_F\right) + \left(\gamma\,\tilde{X}_F + \tilde{X}_F\right)^T\left(M^{-1}\psi_F\right) \tag{51}$$

The product $\left(\gamma\tilde{X}_F + \tilde{X}_F\right)^T sgn\left(\gamma\tilde{X}_F + \tilde{X}_F\right)^T$ is:

$$\left(\gamma\,\tilde{X}_F + \tilde{X}_F\right)^T\left(M^{-1}\psi_F\right) = \left\|\gamma\,\tilde{X}_F + \tilde{X}_F\right\|_1 - \eta\varepsilon + \sum_{k=1}^{n}\frac{\varepsilon^2}{\left|\left(\gamma\,\tilde{X}_F + \tilde{X}_F\right)_k\right| + \varepsilon} \geq 0$$

If $0<c<1$ the inequality is met when:

$$\left\|\gamma\tilde{X}_F + \dot{\tilde{X}}_F\right\|_1 > \frac{\eta\varepsilon}{c} \tag{52}$$

$$\left(\gamma\,\tilde{X}_F + \tilde{X}_F\right)^T \operatorname{sgn}\left(\gamma\,\tilde{X}_F + \tilde{X}_F\right) > (1-c)\left\|\gamma\,\tilde{X}_F + \tilde{X}_F\right\|_1$$

$$\dot{V} < -\begin{bmatrix}\tilde{X}_F^T & \tilde{X}_F^T\end{bmatrix} Q - \left\|\gamma\,\tilde{X}_F + \tilde{X}_F\right\|_1\left[\beta(1-c) - \left\|M^{-1}\psi_F\right\|_1\right] \tag{53}$$

To guarantee that $V<0$, the following condition must be met:

$$\beta > \frac{\left\|M^{-1}\psi_F\right\|_1}{1-c} \tag{54}$$

Thus $\tilde{X}_F \to 0$ when $t \to 0$. Considering the same analysis for $\tilde{Y}_F$, it is obtained that $\tilde{Y}_F \to 0$ the same stability analysis is developed for the Y-axis.

4- Test and Results

To validate the hybrid control, two experiments have been developed: i) formation of 7 robots (4 leaders and three followers), and ii) formation of 12 robots (4 leaders and eight followers). With these experiments, it is intended to demonstrate that with the proposed hybrid controller, it is possible to make the scalability of a null space algorithm for a formation of mobile robots, maintaining the structure of the controller despite increasing the number of robots, it is also intended to verify that there are no singularities in the formation of the robot followers. And the convergence to zero of the control errors will be verified. The main advantage of the proposal is that the formation of the followers does not depend on any geometric shape. The controller parameters are $K_f=3.8$; $K_{f1}=5.5$; $K_p=2.8$; $k_{p1}=10.5$; $\alpha=10$; $\gamma=30$; $\beta=7$, these values were obtained empirically through experimentation. In the first experiment, seven robots are considered. The distribution of robots is shown in Figure 8.

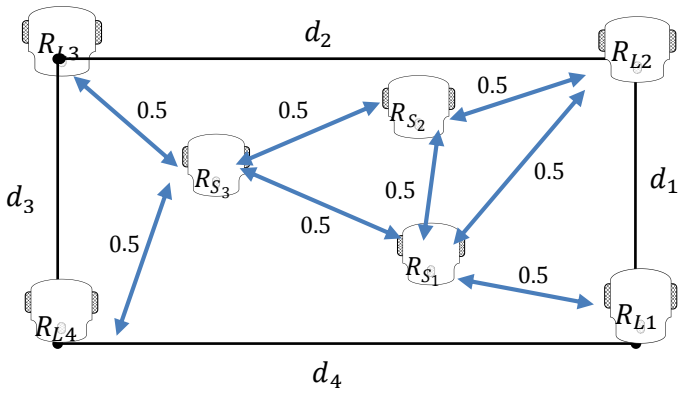

Figure 8. Distribution of the formation of leaders and followers

From Figure 8, the Laplacian Matrix is given by:

$$\Gamma = \begin{bmatrix} 0 & 0 & 0 & 0 & 0 & 0 & 0 \\ 0 & 0 & 0 & 0 & 0 & 0 & 0 \\ 0 & 0 & 0 & 0 & 0 & 0 & 0 \\ 0 & 0 & 0 & 0 & 0 & 0 & 0 \\ -0.5 & 0 & 0 & -0.5 & 2 & -0.5 & 0.5 \\ 0 & -0.5 & 0 & 0 & -0.5 & 1.5 & -0.5 \\ 0 & 0 & -0.5 & -0.5 & -0.5 & -0.5 & 2 \end{bmatrix} \quad (55)$$

The trajectory is defined by $f(t) = sin(\pi t/4)$, the sampling time is $t_s = 0.02\,s$. Figure 9 shows the trajectory tracking for a group of robots, four leader robots, and three follower robots. The leader robots start from an initial position; the null space control brings the leading robots to a square shape. The follower robots also start from an initial position, and the consensus algorithm control allows the followers robots to be in the desired positions. The centroid of the square formed by the leaders follows the desired sinusoidal trajectory. It can be seen in Figure 9 that the leader robots form a square, and the follower robots are positioned in the desired position of the formation.

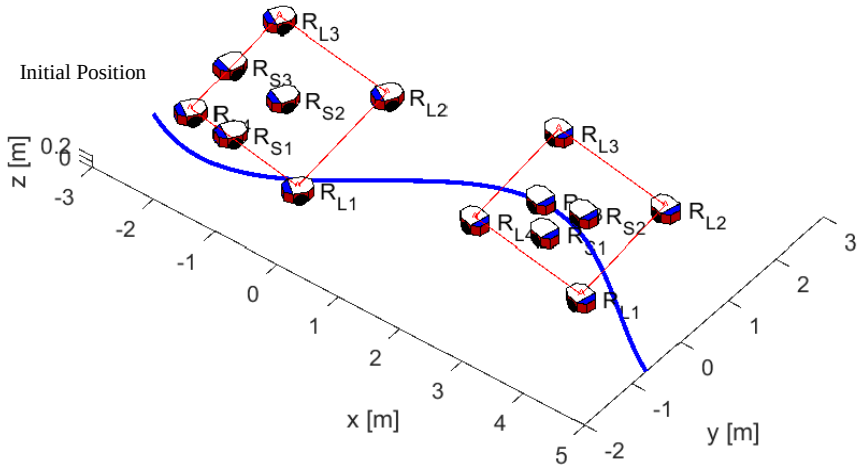

Figure 9. The trajectory of leader robots and follower robots

Figure 10 shows $\tilde{x}_c$ the posture error in X, and $\tilde{y}_c$ the posture error in Y, the initial position of the centroid of the formation of the leader robots starts outside the desired trajectory, for which an error is generated at the time t_0, task 1 of the null_space control takes the centroid of the formation to the desired trajectory; it is observed in the figure that the posture errors converge to zero, verifying the good performance of the null space controller.

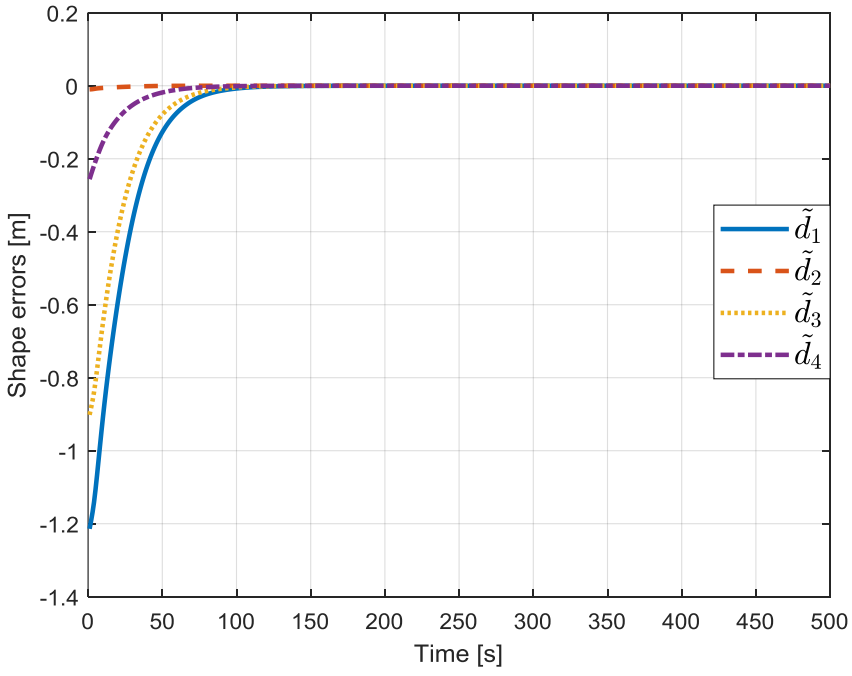

Figure 10. Errors in the posture of the leader

Figure 11 shows the formation errors of the four leader robots $\tilde{d}_1$, $\tilde{d}_2$, $\tilde{d}_3$ and $\tilde{d}_4$. It can be seen that the robots start from an initial position, which generates the formation errors at the time t_0. Task 2 of the null space controller allows the leader robots to form a square figure; it is verified in Figure 11 that the four shape errors converge to zero, which confirms the good performance of the null space controller

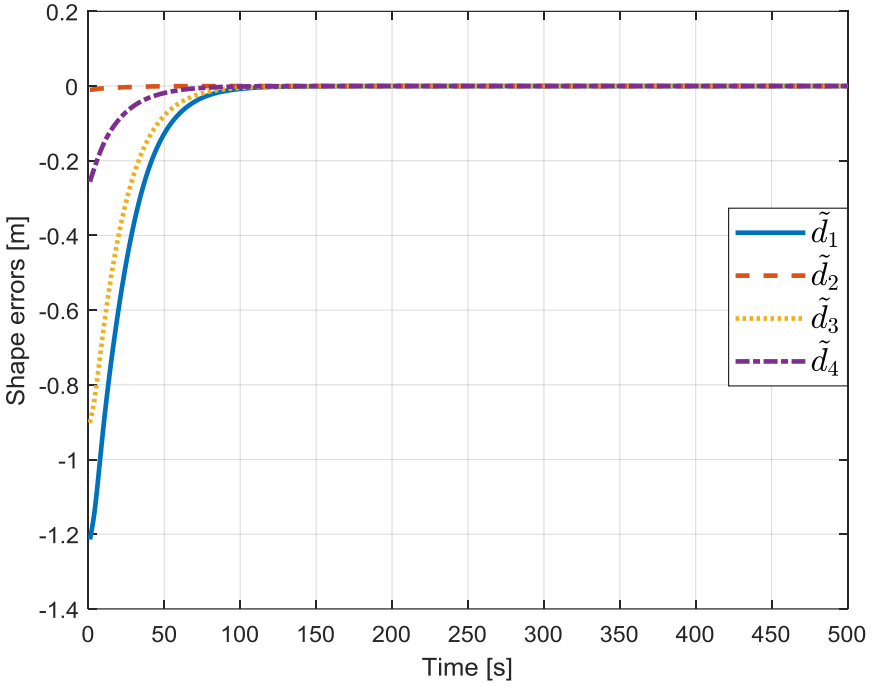

Figure 11. Shape errors of the leader

Figure 12 shows the position errors of the three follower robots, where $\tilde{x}_{S1}, \tilde{x}_{S2}$ and $\tilde{x}_{S3}$ are the position errors in X of the formation of the follower robots $\tilde{y}_{S1}, \tilde{y}_{S2}$ and $\tilde{y}_{S3}$ are the position errors in Y of the formation of the follower robot. To control these errors, the consensus algorithm of the hybrid controller was implemented; it can be seen that the robots start from an initial position different from the desired one, and the consensus algorithm takes the robots to the desired positions. It is verified that the position errors of the follower robots converge to zero, affirming the good behavior of the proposed controller.

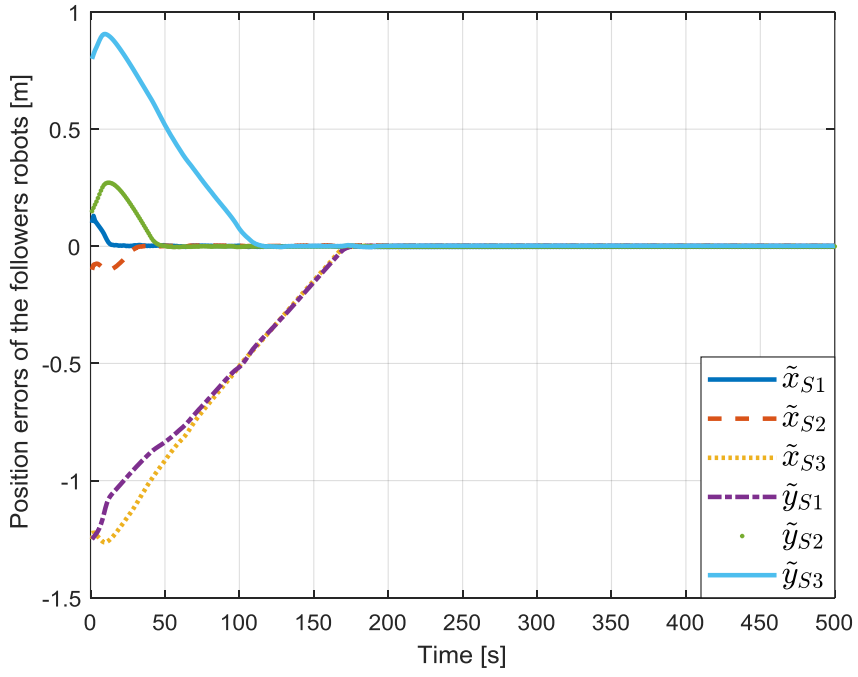

Figure 12. Position errors of the follower robots

In this first experiment, a hybrid controller has been implemented for the formation of 7 robots (4 leader robots and three follower robots); the hybrid controller is structured of the null space controller and a consensus algorithm. As a result, it has been observed that the null space controller meets the posture objectives, the consensus algorithm meets the control objective of the formation of the follower robots. Therefore, the first experiment can verify that the control objectives are met since the errors converge to zero.

Twelve robots (4 leaders and eight followers) are considered for the second experiment. The leader robots maintain the same square shape as in experiment one. The controller structure does not change, task 1 is maintained as a posture control, and task 2 for the formation of the leader and follower robots, the follower robots use consensus algorithms to maintain their shape. The Jacobian of the robots and the Laplacian matrix are changed to increase the number of robots. The location of the follower robots depends on the Laplacian matrix, and they are located as shown in Figure 13.

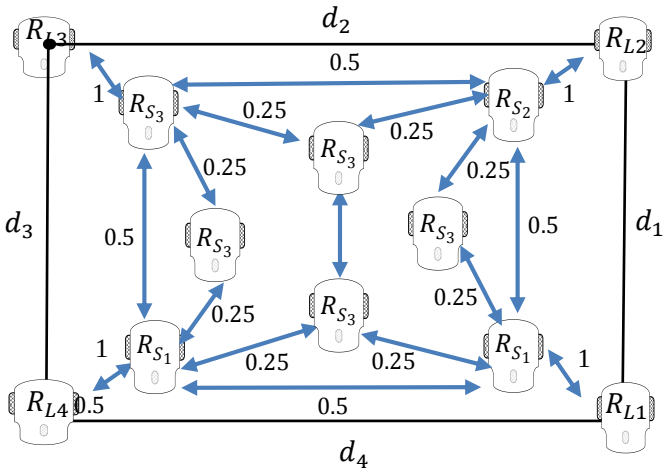

Figure 13. Formation of eight follower robots

From Figure 13, the Laplacian Matrix is given by:

$$\Gamma = \begin{bmatrix} 0 & 0 & 0 & 0 & 0 & 0 & 0 & 0 & 0 & 0 & 0 & 0 \\ 0 & 0 & 0 & 0 & 0 & 0 & 0 & 0 & 0 & 0 & 0 & 0 \\ 0 & 0 & 0 & 0 & 0 & 0 & 0 & 0 & 0 & 0 & 0 & 0 \\ 0 & 0 & 0 & 0 & 0 & 0 & 0 & 0 & 0 & 0 & 0 & 0 \\ -1 & 0 & 0 & 0 & 2.5 & -0.5 & 0 & -0.5 & -0.25 & 0 & -0.25 & 0 \\ 0 & -1 & 0 & 0 & -0.5 & 2.5 & -0.5 & 0 & 0 & -0.25 & -0.25 & 0 \\ 0 & 0 & -1 & 0 & 0 & -0.5 & 2.5 & -0.5 & 0 & -0.25 & 0 & -0.25 \\ 0 & 0 & 0 & -1 & -0.5 & 0 & -0.5 & 2.5 & -0.25 & 0 & 0 & -0.25 \\ 0 & 0 & 0 & 0 & -0.25 & 0 & 0 & -0.25 & 0.75 & -0.25 & 0 & 0 \\ 0 & 0 & 0 & 0 & 0 & -0.25 & -0.25 & 0 & -0.25 & 0.75 & 0 & 0 \\ 0 & 0 & 0 & 0 & -0.25 & -0.25 & 0 & 0 & 0 & 0 & 0.5 & 0 \\ 0 & 0 & 0 & 0 & 0 & 0 & -0.25 & -0.25 & 0 & 0 & 0 & 0.5 \end{bmatrix} \quad (56)$$

Figure 14 shows the trajectory tracking for a group of robots, four leader robots, and eight follower robots. The leader robots start from an initial position; the null space control brings the leading robots to a square shape. The follower robots also start from an initial position, and the consensus algorithm control allows the follower robots to be in the desired positions. The centroid of the square formed by the leaders follows the desired sinusoidal trajectory. It can be seen in Figure 14 that the leader robots form a square, and the follower robots are positioned in the desired position of the formation.

Figure 15 shows $\tilde{x}_c$ the posture error in X, and $\tilde{y}_c$ the posture error in Y, the initial position of the centroid of the formation of the leader robots starts outside the desired trajectory, for which an error is generated at the time t_0Task 1 of the null space control takes the centroid of the formation to the desired trajectory; it is observed in the figure that the posture errors converge to zero, verifying the good performance of the null space controller.

Figure 16 shows the formation errors of the four leader robots $\tilde{d}_1$, $\tilde{d}_2$, $\tilde{d}_3$ and $\tilde{d}_4$. It can be seen that the robots start from an initial position, which generates the formation errors at the time t_0. Task 2 of the null space controller allows the leader robots to form a square figure; it is verified in the figure that the four shape errors converge to zero, which verifies the good performance of the null space controller.

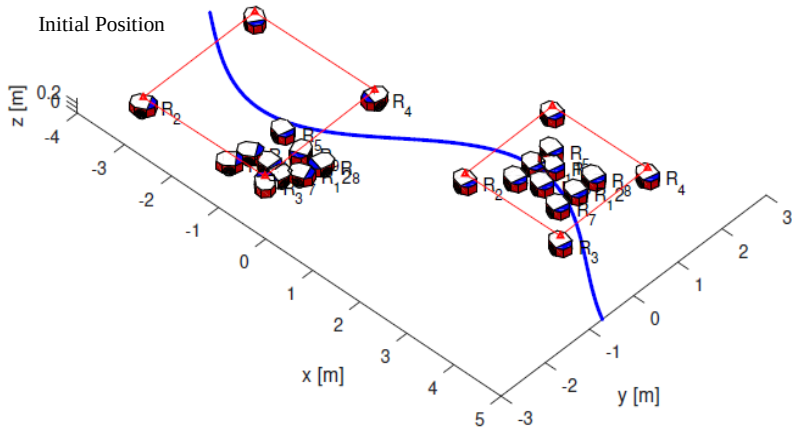

Figure 14. **The trajectory of the leader robots and following robots**

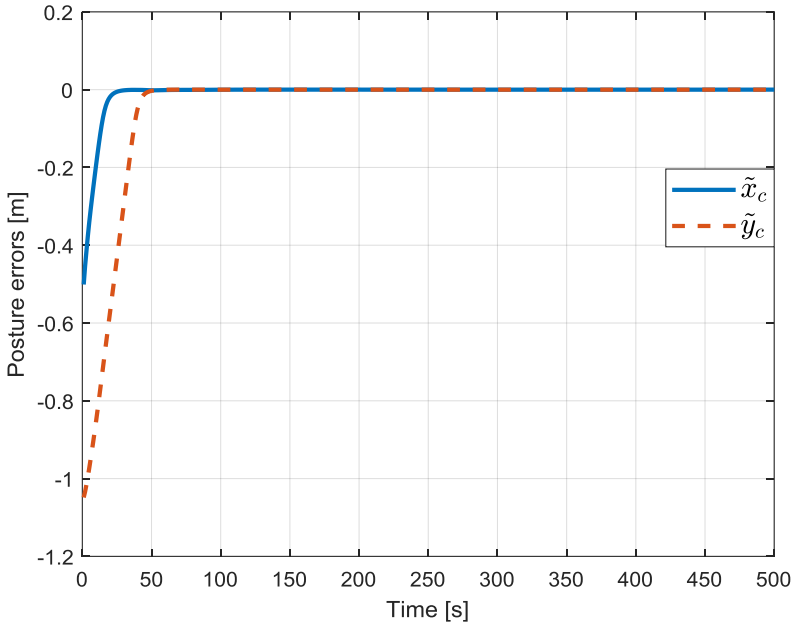

Figure 15. **Errors in the posture of the leaders**

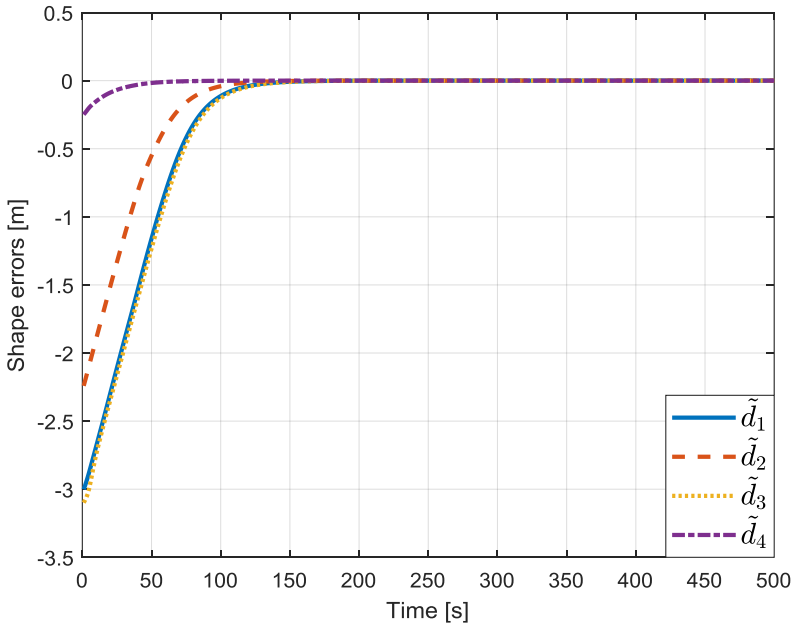

Figure 16. **Shape errors of the leaders**

Figures 17 and 18 show the position errors of the eight follower robots, where $\tilde{x}_{S1}, \tilde{x}_{S2}, \tilde{x}_{S3}, \tilde{x}_{S4}, \tilde{x}_{S5}, \tilde{x}_{S6}, \tilde{x}_{S7}$ *and* $\tilde{x}_{S8}$ are the position errors in X of the formation of the follower robots $\tilde{y}_{S1}, \tilde{y}_{S2}, \tilde{y}_{S3}, \tilde{y}_{S4}, \tilde{y}_{S5}, \tilde{y}_{S6}, \tilde{y}_{S7}$ *and* $\tilde{y}_{S8}$ are the position errors in Y of the formation of the follower robot. To control these errors, the consensus algorithm of the hybrid controller was implemented; it can be seen that the robots start from an initial position different from the desired one, and the consensus algorithm takes the robots to the desired positions. It is verified that the position errors of the follower robots converge to zero, verifying the good behavior of the proposed controller.

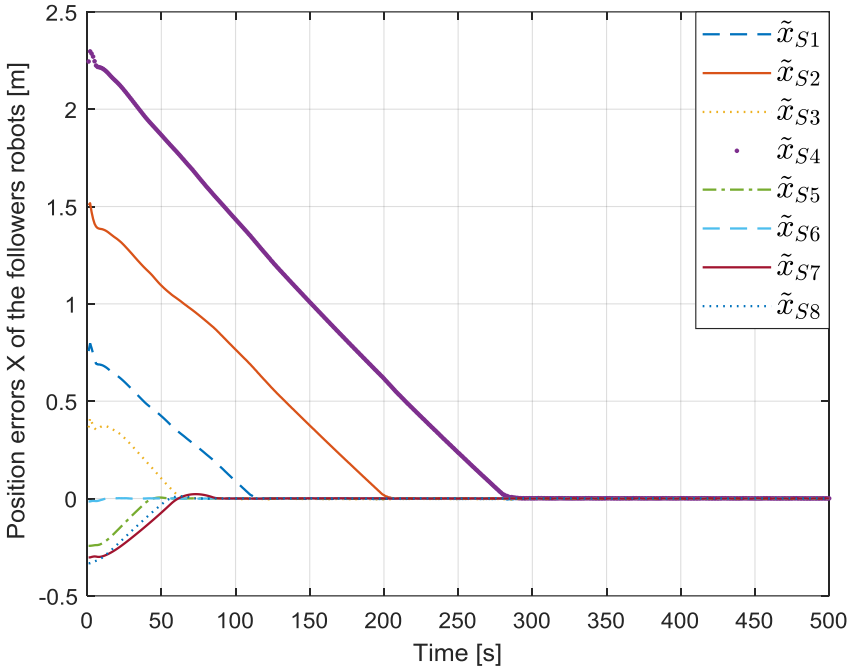

Figure 17. Position errors X of the follower robots

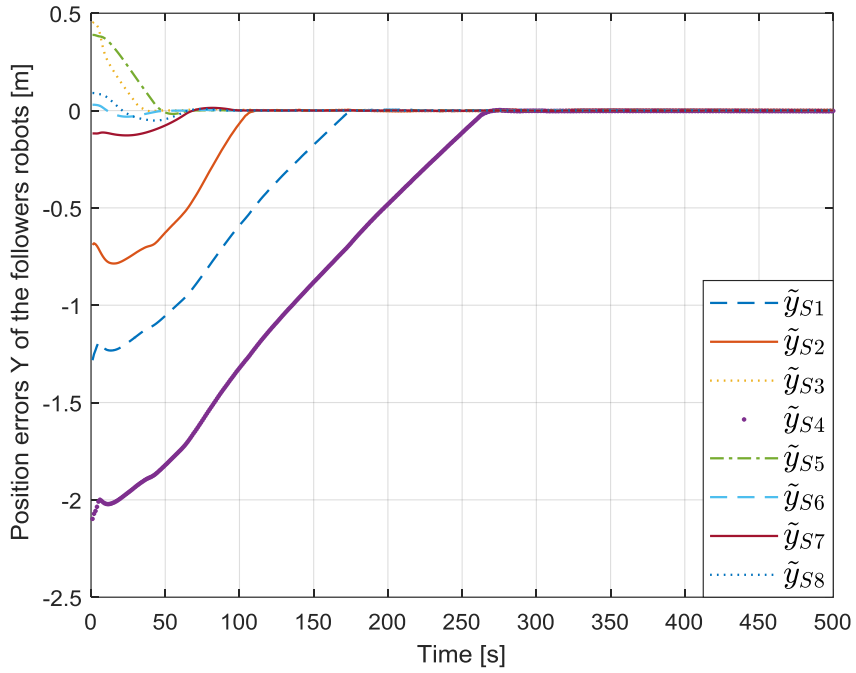

Figure 18. Position errors Y of the follower robots

In this second experiment, a hybrid controller has been implemented for the formation of 12 robots (4 leader robots and eight follower robots); the hybrid controller is structured around the null space controller and a consensus algorithm. The structure of the controller is maintained; what changes is the Laplacian matrix, and it has been observed that the null space controller meets the posture objectives, the consensus algorithm meets the control objective of the formation of the eight follower robots. The second experiment can verify that the control objectives are met since the errors

converge to zero. The scalability of the controller is demonstrated in this second experiment, where it can be verified that the control objectives are met since the errors converge to zero.

Based on the experiments carried out, it can be determined that the hybrid control topology enhances multitasking in the formation of mobile robots regardless of the number of robots. The implementation of the null space algorithm allows a controller with multiple tasks, such as i) the posture task, which allows the formation centroid of the leading robots to follow the desired trajectory, ii) the shape task, which allows the leading robots to form a square, and iii) in the task of forming the following robots, the advantages of the consensus algorithm are included, such as the formation of the follower robots as a task within the null space does not depend on a geometric figure, so it is not necessary to redesign the controller, introducing scalability to the null space, adding advantages to the hybrid proposal, singularities that can be generated in certain configurations are avoided. This proposal combines the best features of null space control and consensus algorithms.

5- Conclusion

In the present work, a novel proposal for a hybrid control based on null-space and consensus algorithms to solve the scalability problem of robot formation was developed. The main advantage of the proposal is that the formation of the followers does not depend on any geometric shape. Simulation tests have shown the outstanding performance of the proposed controller in the formation of non-holonomic mobile robots, and the algorithm scalability has been validated. Furthermore, the performed tests showed that the errors of the three tasks in the null space converged to zero: i) the leader position task, ii) the leader shape task, and iii) the follower formation task. Furthermore, the results confirmed that the controller structure did not change despite increasing or decreasing the number of follower robots in the formation. Based on the experiments carried out, it can be determined that the hybrid control topology enhances multitasking in the formation of mobile robots regardless of the number of robots.

Furthermore, the formation of the follower robots as a task within the null space does not depend on a geometric figure, so it is not necessary to redesign the controller, introducing scalability to the null space, adding advantages to the hybrid proposal. Another advantage of implementing this structure is that it differs from algorithms based on geometric figures in that it does not introduce singularities in the formation of mobile robots. Therefore, the approach presented a control algorithm that allows the null space and consensus algorithms to solve the scalability problem and the geometric shape dependence for the follower robots' formation. In future work, it is proposed to analyze a complete model of the robots in which changes in the dynamics are considered to develop an in-depth study of the performance of the proposed controller.

6- Declarations

6-1- Author Contributions

G.A.: Conceptualization, Methodology, Analysis, Software, Writing - original draft. P.L.: Conceptualization, Methodology, Analysis, Supervision. M.H.: Conceptualization, Analysis, Writing. L.M.: Methodology, Analysis, Software. O.C.: Conceptualization, Methodology, Analysis, Supervision. All authors have read and agreed to the published version of the manuscript.

6-2- Data Availability Statement

The data presented in this study are available on request from the corresponding author.

6-3- Funding and Acknowledgements

This work was sponsored by Universidad Internacional del Ecuador, Escuela Politécnica Nacional and Universidad San Francisco de Quito. PL, MH, and LM thank the PIS-19-10 Project of the Escuela Politécnica Nacional for their sponsorship to realize this work.

6-4- Conflicts of Interest

The author declares that there is no conflict of interest regarding the publication of this manuscript. In addition, the ethical issues, including plagiarism, informed consent, misconduct, data fabrication and/or falsification, double publication and/or submission, and redundancies have been ultimately observed by the authors.

7- References

[1] Tanner, H. G., Pappas, G. J., & Kumar, V. (2004). Leader-to-formation stability. IEEE Transactions on robotics and automation, 20(3), 443-455. doi: 10.1109/TRA.2004.825275.

[2] Oh, K. K., Park, M. C., & Ahn, H. S. (2015). A survey of multi-agent formation control. Automatica, 53, 424–440. doi:10.1016/j.automatica.2014.10.022.

[3] Claret, J.-A. (2019). The Robot Null Space: New Uses for New Robotic Systems. PhD Dissertation, Technical university of Catalonia Barcelona tech, Barcelona, Spain.

[4] Martinez, J. B., Becerra, H. M., & Gomez-Gutierrez, D. (2021). Formation tracking control and obstacle avoidance of unicycle-type robots guaranteeing continuous velocities. Sensors, 21(13), 4374. doi:10.3390/s21134374.

[5] Rashid, M. Z. A., Yakub, F., Zaki, S. A., Ali, M. S. M., Mamat, N. M., Mohd Putra, S. M. S., Roslan, S. A., Shah, H. N. M., & Aras, M. S. M. (2019). Comprehensive review on controller for leader-follower robotic system. Indian Journal of Geo-Marine Sciences, 48(7), 985–1007.

[6] Saradagi, A., Muralidharan, V., Krishnan, V., Menta, S., & Mahindrakar, A. D. (2018). Formation Control and Trajectory Tracking of Nonholonomic Mobile Robots. IEEE Transactions on Control Systems Technology, 26(6), 2250–2258. doi:10.1109/TCST.2017.2749563.

[7] Antonelli, G., Arrichiello, F., & Chiaverini, S. (2008). The null-space-based behavioral control for autonomous robotic systems. Intelligent Service Robotics, 1(1), 27–39. doi:10.1007/s11370-007-0002-3.

[8] Antonelli, G., Arrichiello, F., & Chiaverini, S. (2009). Experiments of formation control with multirobot systems using the null-space-based behavioral control. IEEE Transactions on Control Systems Technology, 17(5), 1173–1182. doi:10.1109/TCST.2008.2004447.

[9] Rosales, C., Leica, P., Sarcinelli-Filho, M., Scaglia, G., & Carelli, R. (2016). 3D Formation Control of Autonomous Vehicles Based on Null-Space. Journal of Intelligent and Robotic Systems: Theory and Applications, 84(1–4), 453–467. doi:10.1007/s10846-015-0329-5.

[10] Trujillo, M. A., Becerra, H. M., Gómez-Gutiérrez, D., Ruiz-León, J., & Ramírez-Treviño, A. (2018). Priority Task-Based Formation Control and Obstacle Avoidance of Holonomic Agents with Continuous Control Inputs. IFAC-PapersOnLine, 51(13), 216–222. doi:10.1016/j.ifacol.2018.07.281.

[11] Leica, P., Herrera, M., Rosales, C., Roberti, F., Toibero, J., & Carelli, R. (2018). Dynamic obstacle avoidance based on time-variation of a potential field for robots formation. IEEE 2nd Ecuador Technical Chapters Meeting, ETCM 2017, Salinas, Ecuador, 1–6. doi:10.1109/ETCM.2017.8247493.

[12] Arevalo, B., Cruz, P. J., & Leica, P. (2018). Sliding mode formation control of mobile robots with input delays. IEEE 2nd Ecuador Technical Chapters Meeting, ETCM 2017, Salinas, Ecuador, 1–6. doi:10.1109/ETCM.2017.8247448.

[13] Fan, J., Liao, Y., Li, Y., Jiang, Q., Wang, L., & Jiang, W. (2019). Formation Control of Multiple Unmanned Surface Vehicles Using the Adaptive Null-Space-Based Behavioral Method. IEEE Access, 7, 87647–87657. doi:10.1109/ACCESS.2019.2925466.

[14] Camacho, O., Leica, P., Antamba, J., & Quinonez, J. (2019). Null-Space Based Control Applied to a Formation of Aerial Manipulators in Congested Environment. Proceedings - 2019 International Conference on Information Systems and Computer Science, INCISCOS 2019, Quito, Ecuador, 244–250. doi:10.1109/INCISCOS49368.2019.00046.

[15] Moreira, M. S. M., Brandao, A. S., & Sarcinelli-Filho, M. (2019). Null space based formation control for a UAV landing on a UGV. 2019 International Conference on Unmanned Aircraft Systems, ICUAS 2019, Atlanta, United States, 1389–1397. doi:10.1109/ICUAS.2019.8797820.

[16] Samaniego, P., Vaca, E., Leica, P., Chavez, D., & Camacho, O. (2018). Dynamic obstacle avoidance based on null-space for quadcopter's formation. IEEE 2nd Ecuador Technical Chapters Meeting, ETCM 2017, Salinas, Ecuador, 1–6. doi:10.1109/ETCM.2017.8247532.

[17] Vaca, E., Samaniego, P., Cruz, P. J., & Leica, P. (2019). Null-Space based Robust Controller for Quadcopter's formation in windy environments. Proceedings - 3rd IEEE International Conference on Robotic Computing, IRC 2019, Naples, Italy, 643–649. doi:10.1109/IRC.2019.00131.

[18] Bacheti, V. P., Brandão, A. S., & Sarcinelli-Filho, M. (2021). Path-following by a UGV-UAV formation based on null space. 2021 14th IEEE International Conference on Industry Applications, INDUSCON 2021 - Proceedings, Sao Paulo, Brazil, 1266–1273. doi:10.1109/INDUSCON51756.2021.9529472.

[19] Neto, V. E., Sarcinelli-Filho, M., & Brandao, A. S. (2019). Trajectory-tracking of a heterogeneous formation using null space-based control. 2019 International Conference on Unmanned Aircraft Systems, ICUAS 2019, Atlanta, United States, 187–195. doi:10.1109/ICUAS.2019.8798031.

[20] Huang, Y. C., Shen, J. T., Chiang, M. L., Chen, Y. W., Chua, T. L., & Fu, L. C. (2019). Dual Null-Space Based Controller Design with Signal Compensation for Formation with Conflicted Tasks. CCTA 2019 - 3rd IEEE Conference on Control Technology and Applications, City University of Hong Kong, Hong Kong, China, 958–963. doi:10.1109/CCTA.2019.8920433.

[21] Zhou, N., Cheng, X., Xia, Y., & Liu, Y. (2020). Distributed Formation Control of Multi-Robot Systems: A Fixed-Time Behavioral Approach. 59th IEEE Conference on Decision and Control, CDC 2020, Jeju Island, South Korea, 4017–4022. doi:10.1109/CDC42340.2020.9304057.

[22] Olfati-Saber, R., Fax, J. A., & Murray, R. M. (2007). Consensus and cooperation in networked multi-agent systems. Proceedings of the IEEE, 95(1), 215–233. doi:10.1109/JPROC.2006.887293.

[23] Ren, W., & Beard, R. W. (2008). Distributed consensus in multi-vehicle cooperative control: Theory and applications. Communications and Control Engineering, London, United Kingdom. doi: 10.1007/978-1-84800-015-5.

[24] Ren, W., & Cao, Y. (2011). Distributed coordination of multi-agent networks: Emergent problems, models, and issues. In Communications and Control Engineering, Springer, London, United Kingdom. doi:10.1007/978-0-85729-169-1.

[25] Zhang, H., Zhao, Z., Meng, Z., & Lin, Z. (2014). Experimental verification of a multi-robot distributed control algorithm with containment and group dispersion behaviors: The case of dynamic leaders. IEEE/CAA Journal of Automatica Sinica, 1(1), 54–60. doi:10.1109/JAS.2014.7004620.

[26] Cao, Y., Stuart, D., Ren, W., & Meng, Z. (2010). Distributed containment control for double-integrator dynamics: Algorithms and experiments. Proceedings of the 2010 American Control Conference, Baltimore, United States, 3830-3835.

[27] Cao, Y., Ren, W., & Egerstedt, M. (2012). Distributed containment control with multiple stationary or dynamic leaders in fixed and switching directed networks. Automatica, 48(8), 1586–1597. doi:10.1016/j.automatica.2012.05.071.

[28] Vizuete, R., Abad Torres, J., Leica, P. (2020). Application of a Distributed Containment Algorithm: Trajectory Tracking for Mobile Robots. In: Gusikhin, O., Madani, K. (eds) Informatics in Control, Automation and Robotics. ICINCO 2017. Lecture Notes in Electrical Engineering, vol 495. Springer, Cham, Switzerland. doi: 10.1007/978-3-030-11292-9_11.

[29] Peng, H., Wang, J., Wang, S., Shen, W., Shi, D., & Liu, D. (2020). Coordinated Motion Control for a Wheel-Leg Robot with Speed Consensus Strategy. IEEE/ASME Transactions on Mechatronics, 25(3), 1366–1376. doi:10.1109/TMECH.2020.2975083.

[30] Koung, D., Fantoni, I., Kermorgant, O., & Belouaer, L. (2020). Consensus-based formation control and obstacle avoidance for nonholonomic multi-robot system. 16th IEEE International Conference on Control, Automation, Robotics and Vision, ICARCV 2020, Shenzhen, China, 92–97. doi:10.1109/ICARCV50220.2020.9305426.

[31] Wang, N., Dai, J., & Ying, J. (2021). Research on Consensus of UAV Formation Trajectory Planning Based on Improved Potential Field. 40th Chinese Control Conference, CCC, Shanghai, China, 99–104. doi:10.23919/CCC52363.2021.9550138.

[32] Xu, Y., Yao, F., & Chai, S. (2020). Distributed Formation Control for Multiple Quadrotor System Based on Consensus Algorithm. 39th Chinese Control Conference, CCC, 2020-July, Shenyang, China, 4872–4877. doi:10.23919/CCC50068.2020.9189136.

[33] Wu, F., He, J., Zhou, G., Li, H., & Liu, Y. (2021). Performance of Sliding Mode and Consensus-based Control Approaches for Quadrotor Leader-Follower Formation Flight. 2021 International Conference on Unmanned Aircraft Systems, ICUAS 2021, Athens, Greece, 1671–1676. doi:10.1109/ICUAS51884.2021.9476782.

[34] Kada, B., Khalid, M., & Shaikh, M. S. (2020). Distributed cooperative control of autonomous multi-Agent UAV systems using smooth control. Journal of Systems Engineering and Electronics, 31(6), 1297–1307. doi:10.23919/JSEE.2020.000100.